SCA-9919

PERMEABILITY MAPPING ON VUGGY CORE SAMPLE USING TRACER EXPERIMENTS AND STREAM-LINE SIMULATIONS.

Andrés Moctezuma-B.[1] and Marc Fleury[2]

[1] Instituto Mexicano del Petróleo, México, [2]Institut Français du Pétrole, France.

Abstract

Carbonate rocks have complex porous structure and conventional approach to characterize two phase flow in the laboratory can be inadequate, especially in vuggy structures. Various laboratory studies indicate that centimeter scale heterogeneities have important effects. An important question is the determination of the 3D permeability map later used in the interpretation of two phase flow experiments.

Our approach is based on the combined use CT scan 3D porosity maps, NMR relaxometry, tracer experiments and numerical simulations to derive a 3D permeability map consistent with the experimental observations. NMR T2 measurements are used to quantify the average porous volume represented by the vugs while CT scan can reproduce the spatial distribution of porosity at the millimeter scale. The permeability map is mainly deduced by fitting the tracer experiment using 3D numerical simulations where we introduce the CT scan porosity map and where the permeability in each grid cell take only two values, one associated with vugs, and one with the matrix.

The study was performed using a volcanic rock (Andesite) with 22% porosity and low permeability (0.4 mD) to mimic a non fractured vuggy carbonate. The variogram analysis in the flow direction does not indicate a correlation of the porosity map. However, the tracer experiment indicates the existence of a preferential path and the measured flux dispersion behaves as in a layered system (early breakthrough, long tail). For a given volume fraction of vugs (congruent with NMR results), the experiments can be reproduced with numerical simulation by adjusting the permeability contrast between the matrix and vug to 360. The use of a streamline simulator was necessary because of the large number of grid cells used and low numerical dispersion. Finally, miscible displacement experiments using different viscosity fluids are interpreted and discussed using three models considering heterogeneity and viscosity.

Introduction

There is considerable work on miscible displacements in porous media both experimentally and theoretically. In particular, tracer experiments, a displacement of a fluid by another miscible fluid with the same viscosity, can be used to estimate the degree of heterogeneity of a sample in terms of permeability and highlight preferential paths that may be present in the sample studied. As a response to a step injection, the concentration at the outlet will gradually increase due to a dispersion mechanism which has mainly two origins: the hydrodynamic dispersion (mechanical phenomenon), related to the speed of the displacement and, the molecular diffusion between fluids (physicochemical phenomenon).

We focus in this paper only on the hydrodynamic dispersion which is due to a distribution of velocity in the porous space essentially for the following reasons: (i) there is a speed gradient from the surface of the pore to the center as in a capillary tube, (ii) the flow area between pores is not equal, yielding different speeds along the pores and (iii) the stream lines generated in the pores are different to the mean stream line of flow in the sample.

Depending on the importance of the above mechanisms, one will obtain different types of curves, as shown in figure 1. If the sample is homogeneous, the dispersion curve will be due to velocity gradients at the pore level and from standard analysis, one can deduced the pore size or grain size of the sample. If the throat size distribution is large or if the structure is correlated (e.g. lamination), the dispersion curve may stay symmetric but with a larger width (weakly heterogeneous, figure 1).

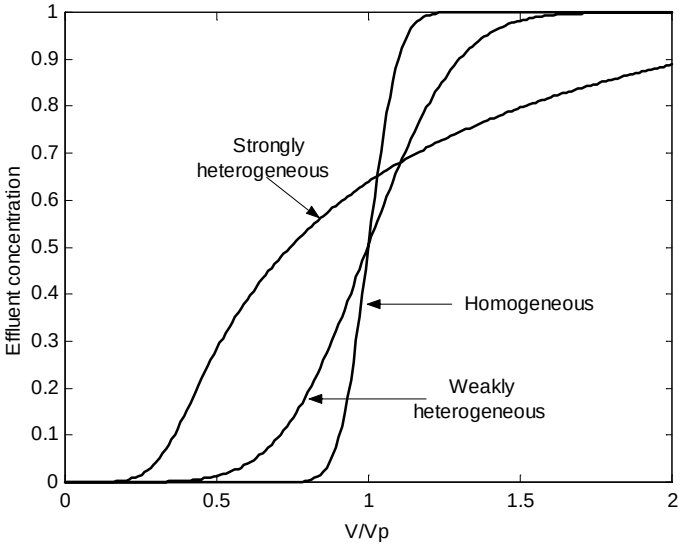

Figure 1 : Effluent dispersion curves are signature of strong of weak heterogeneity.

At the extreme case, a fractured or layered system, for example, will generate preferential paths and the dispersion curve will be strongly non symmetrical with early breakthrough and long tail features (figure 1). With the aim of estimating multiphase flow properties, one can predict that standard analysis for relative permeability determination will not be applicable for strongly heterogeneous systems, and is questionable for the weakly heterogeneous case (deZabala and Kamath, 1995, Bahralolom and Heller, 1992). In the laboratory, there is little attempt to try to use the information obtained in tracer experiment for multiphase flow property determination.

In this paper, we consider the case of 'pure' vugular structure in which the pore space has two populations of pores ranging from 10 micron up to 1 mm. These structures can be found in carbonate rocks with a high degree of dolomitization. As a consequence of other various diagenetic processes, carbonate rocks are often fractured or fissured at various scales, and the matrix can have a very low permeability (0.1 to 10 mD). To study solely the effect of vugs in a dense matrix, we chose a volcanic rock where the vugs are created by a random process.

Sample characterization

The sample studied is a volcanic rock from the Massif Central (Andésite, A6). Similar vugular carbonate rocks were also available but it was difficult to find a long core showing a uniform density of vugs over 20 cm. As will be seen below, the proportion of vugs is similar to carbonate reservoir rocks with strong dissolution processes. The sample was 5 cm in diameter, 20 cm in length with a permeability of 0.5 mD and a porosity of 22%.

CT scan porosity map

CT scanning was performed over the entire length of the sample and 197 slices were taken each 1 mm. The slices have a thickness of 1.3 mm with a pixel resolution of 0.2 mm. The measurements were performed in the cell used for displacement experiment for the dry and saturated sample. Differential CT number images are then calibrated using the measured average porosity by mass balance according to :

$$\left(\phi_{ij}\right)_k = \frac{\overline{\phi_s}}{\overline{\Delta CT_s}} \cdot \left(\Delta CT_{ij}\right)_k \qquad i,j = 1,2,3...257 \quad \text{and} \quad k=1,2,3...197 \tag{1}$$

where subscripts ij indicates the voxel location for each k slice, and s indicates average values for the entire sample. At full CT scan resolution, the final porosity map is described by a matrix of size (257x257x197).

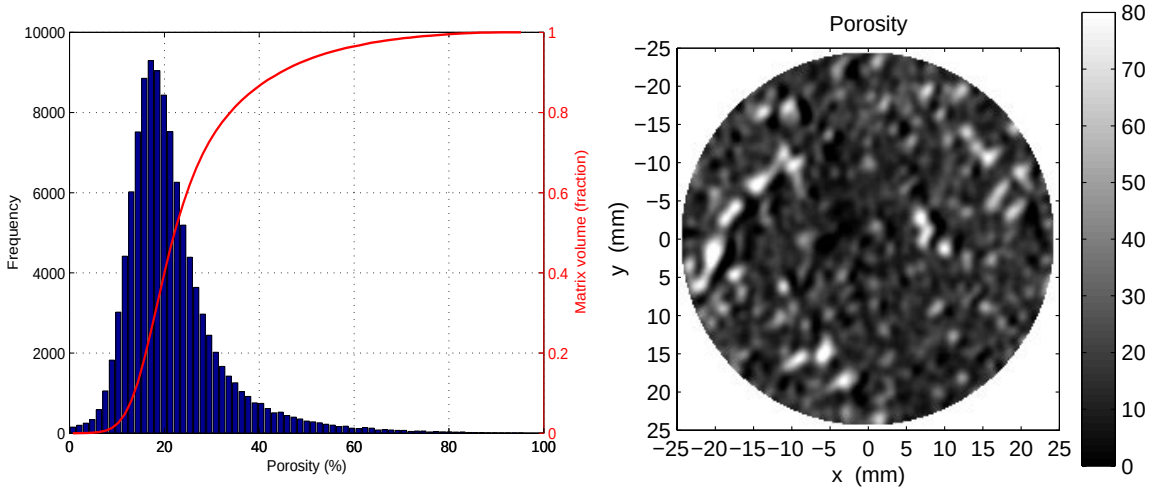

Figure 2 : Porosity distribution from CT scan obtained from 197 images (left). CT scan images show clearly the vugs (left, porosity image for slice 2, scale from 0 to 80 %).

Conventional CT scan voxels are severely distorted in one direction (flow direction) and do not allow a precise measurement of the pore structure. Indeed, the porosity distribution (figure 2) presents a long tail up 100 % saturation, indicating that few vugs are resolved fully. Note that the tail represents a large volume. Nevertheless, the CT scan images indicate clearly (but qualitatively) the vug system.

Variogram analysis

Using the full resolution porosity map (257x257x197), we carried out standard statistical analysis to determine the correlation length of the system. A correlation function γ was computed in the flow direction according to the relation :

$$\gamma(h) = \sum_{i=1}^{n} [\phi(x) - \phi(x+h)]^2 / n \qquad (2)$$

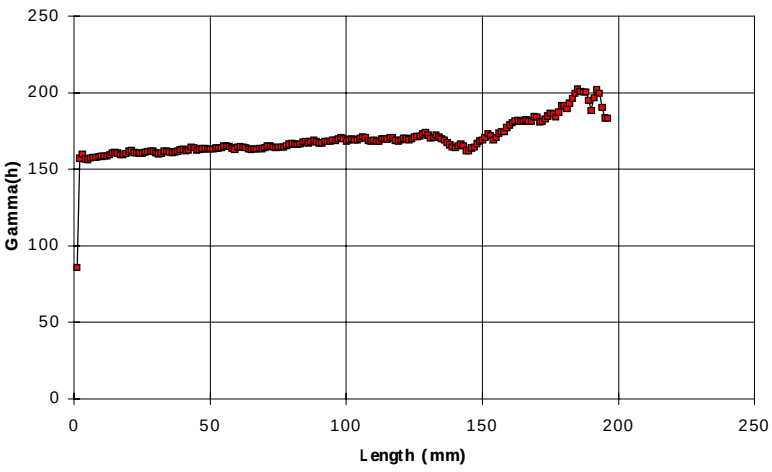

Figure 3 : Correlation function in the flow direction. The gamma function is stable at very small length, indicating that the vug system is not correlated.

where x is a vector location in the core, h the separation distance between pairs of points and n the total numbers of pairs.

The immediate increase of γ at small h (figure 3) indicates that the vug system is not correlated. Oscillations at large h are due to a lack of statistical convergence.

NMR T2 measurements

NMR T2 measurements were performed to evaluate the contribution of the vugs to the total porous volume, which is not possible with CT scan data. We used a MARAN 2 instrument working at 2.2MHz

and we analyzed a sample of length 5 cm cut from the long core studied. NMR T2 measurements can clearly distinguish the vugs and the matrix because of the large contrast of size. The measured relaxation time T2 are related to pore size according to:,

$$T_2^{-1} = T_{2b}^{-1} + \rho / r \qquad \text{(valid on for } \frac{\rho r}{D_m} << 1) \qquad (3)$$

Pore size (r) distributions can be calculated for small pores only. Vugs of typical size of 1 mm (as observed by eye) do not verify the above inequality condition and will therefor have relaxation time that are not proportional to their sizes and are weakly influenced by the surface of the vugs. Hence the vugs will be characterized by the relaxation time of bulk water T2b.

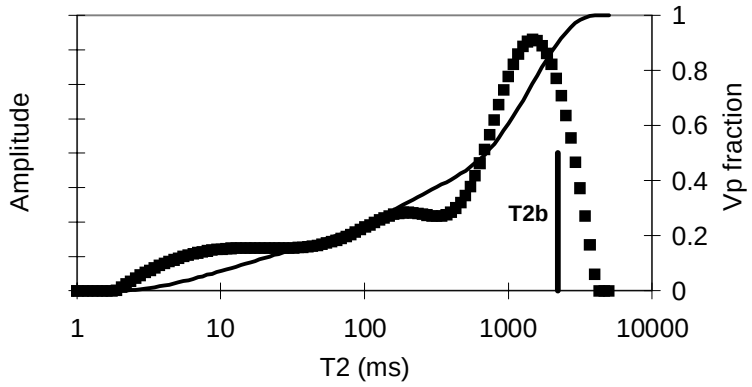

Figure 4 : NMR T2 relaxation time distribution (left scale) and cumulative volume. The vertical line indicates the bulk T2b value. The main peak is the signature of vugs and represents 60% of the total porous volume.

The measured distribution is shown in figure 4. The CPMG signal was acquired using a high signal to noise ratio to avoid uncertainty in the calculation of the T2 distribution and the echo spacing was set to the minimum possible (120 us). The vug population is seen near the value of bulk water (the water saturating the sample) measured separately and the matrix is characterized by relaxation times smaller than 300 ms. The cumulative volume (figure 4) indicates that the vugs represent about 60 % of the total porous volume. This is common in carbonate rock with a high degree of dolomitization and is often coupled with a low permeability. The slight shift between the main peak and the bulk T2 value is not due to measurement errors but to strong internal gradients caused by large quantities of iron (estimated to 5 %) present in this rock. Hence, these gradients were effective even in vugs and FID signals could not be measured with the apparatus (and therefore T1 cannot be measured using conventional sequence). This effect produces an overlapping of the signals of the two populations (increasing the echo spacing leads to a stronger overlapping).

Miscible displacement experiments

Dispersion due to the pore structure can be measured by miscible displacements experiments and yields dynamic information about the degree of heterogeneity of the system. From variogram analysis, one could deduce that the system may behave as weakly heterogeneous system. This is not confirmed.

Fluids and effluent concentration measurements

We used an optical method to measure effluent concentrations at the outlet of the core (figure 5). Therefor, the choice of fluids is conditioned by the measurement technique (Table 1) and a contrast of light absorption must be present within the two miscible fluids considered. When the sample is saturated with water (fluid 1), fluid 2 is a mixture of water and potassium iodide (KI at a concentration of about 22 ppm) and the measurement is performed at 220 nm. When the sample is (fully) saturated with refined oil, fluid 1 and fluid 2 are various combinations of Soltrol, Dodecane, Marcol 52, as listed in table 1, and the measurements are performed at 260 nm. For each miscible fluid pair, a calibration curve is prepared. For the water system, there is a small non-linearity whereas for the oil system, calibration curves are linear.

Table 1.- Fluids and experimental conditions

#Exp.	Rate	Initial Fluid	Injected Fluid	Viscosity	Density
1	60 cc/hr	Brine 30gr/lt	Brine 30 gr/lt + KI at 22 ppm.	1/1	1.03/1.03
2	60 cc/hr	Brine 30gr/l t+ KI at 22 ppm.	Brine 30gr/lt	1/1	1.03/1.03
3	20 cc/hr	Soltrol	Dodecane	1.55/1.38	0.762/0.750
4	20 cc/hr	Dodecane	Soltrol	1.38/1.55	0.750/0.762
5	20 cc/hr	Soltrol	Marcol52/Dodecane (68:32)	1.55/4.42	0.762/0.794
6	20 cc/hr	Marcol52/Do-decane(68:32)	Soltrol	4.42/1.55	0.794/0.762

Cell and experimental procedure

We used standard equipment to perform the measurements. Special attention has been paid to the injection conditions. Inlet and outlet are equipped with concentric circles (a modified spiral) and the surface of injection covers 50% of the sample face, equally distributed. This set-up allows also a flushing of initial fluid saturating the sample at both faces.

Figure 5: Schematic of the experimental set-up. Injection end-pieces are equipped with spirals to flush both inlet and outlet line. The outlet line is as short as possible. A confining pressure of 55 Bar was applied.

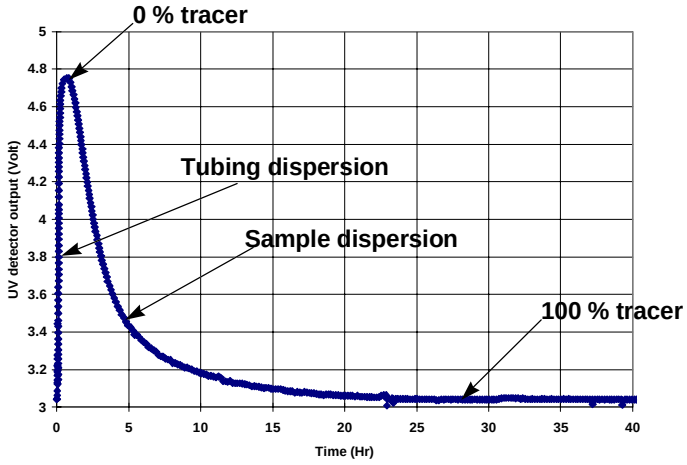

Figure 6: Effluent concentration measurement

The experiments were carried out at laboratory conditions of pressure and temperature (1 bar outlet pressure and 21ºC), and the confining pressure was set to 55 Bars in order to avoid fluid channeling between the sleeve and the core.

The experimental procedure allows an easy and precise calibration to be performed. If fluid 1 is saturating the sample, all the lines and end-pieces are saturated with fluid 2. Then, the experiment is started (figure 6) and the dispersion of the tubes between the outlet face and the detector is first measured. The 0% tracer is determined along with the dead volume at this step. Then the fluids going through the sample is analyzed. At large time, the experiment is stopped when the 10O% level is reached, as measured at the beginning of the experiment.

Results

The results are summarized in figure 7. With the combination of fluids listed in table 1, the density ratios are 1 for water and around 0.9 for oil based fluids. Due to the very low permeability of the sample, the small density difference can be ignored. Viscosity ratio varied from 0.3 up to 3. All the curves were corrected for dead volume and when necessary, for non-linear calibration curves.

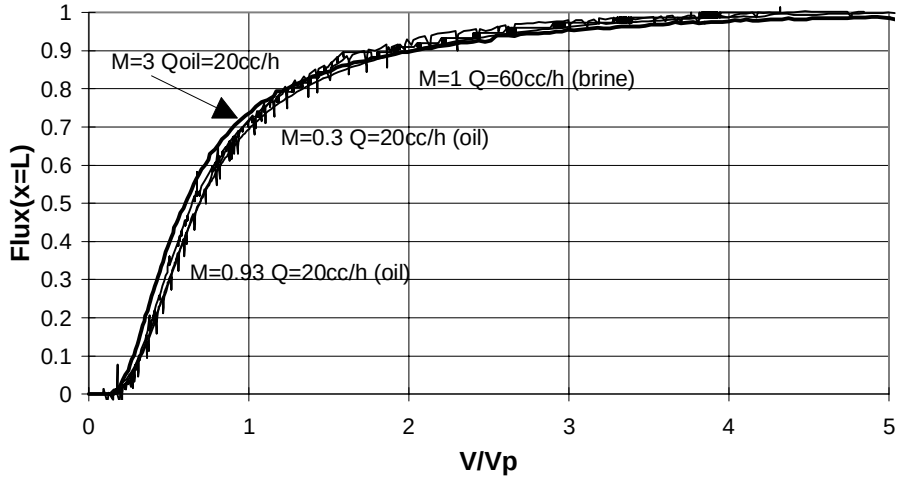

Figure 7: Measured dispersion curves for various flow rates and viscosity ratio (see table 1). The curves are nearly identical.

The various curves are nearly identical (figure 7) and show a preferential path. The breakthrough occurs at about 0.25 V/Vp and there is a long tail behavior. This type of curves is usually obtained for layered system.

Streamline simulations

The objective of these simulations is to reproduce the experiments by adjusting the permeability map, inferred from the porosity map using a given relation between porosity an permeability for each grid cell. The key feature of the streamline simulator used (3DSL, Batycky et al., 1996) is that fluid transport occurs on a streamline grid rather than between the discrete grid blocks on which the pressure field is solved. Because fluid transport is decoupled from the underlying grid (3D transport problem in multiple 1D), the method is computationally efficient and very large time steps can be taken without loss in solution accuracy. Another problem in miscible displacement simulations is the numerical dispersion, which is minimized in this type of simulators because of analytical solutions along streamlines. Various dispersion models are available in the simulator for the dispersion in each stream line and we chose a step function.

We made some tests using conventional finite-difference simulator and the CPU times were not practical (3 days for 1 hour of experimental time against only 25 minutes for 6 hours of experimental time with 3DSL). Therefor, streamline simulation is the best tool in this particular case.

Porosity and permeability maps for numerical simulations

We modified the CT scan porosity map in order to get cubic cells of size 1.8x1.8x1.5 mm approximately. The use of full resolution maps would first enhance one direction and second, yield a very large amount of grid cells (about 8 million active cells). The data describing the core are embedded in a matrix of size 27*27*197 where only 107,365 cells are active (a porosity different from zero) because of the cylindrical shape of the sample.

Table 2.- From porosity to permeability map using a cut-off value in the porosity distribution

Porosity cut off (%)	Volume of vugs (% of Vp)	Number of Kv cells (% of total)
0.15	87.85	77.95
0.20	63.61	47.64
0.21	58.49	42.16
0.22	53.61	37.20
0.23	49.15	32.86
0.25	41.46	25.83
0.28	32.23	18.19

The permeability map is based on the porosity map with the following transform: cells with a porosity higher than a given cut-off will have a high permeability Kv because they contain a large fraction of vugs and cells with a porosity lower than this cut-off value will have a low permeability Km. Table 2 list values of interest extracted from figure 2. A volume fraction of vug of about 60 % (NMR measurements) is retrieved if the porosity cut-off value is set to 0.20. Figure 8 shows a longitudinal cross section of the permeability field obtained in the case of a cut-off value of 0.20.

Simulations were performed using various values of Kv and Km and keeping the average permeability constant. However, the average permeability has no effect on the dispersion curves when expressed as a function of non-dimensional time V/Vp. The boundary conditions for the model were constant inlet flow rate and constant outlet pressure.

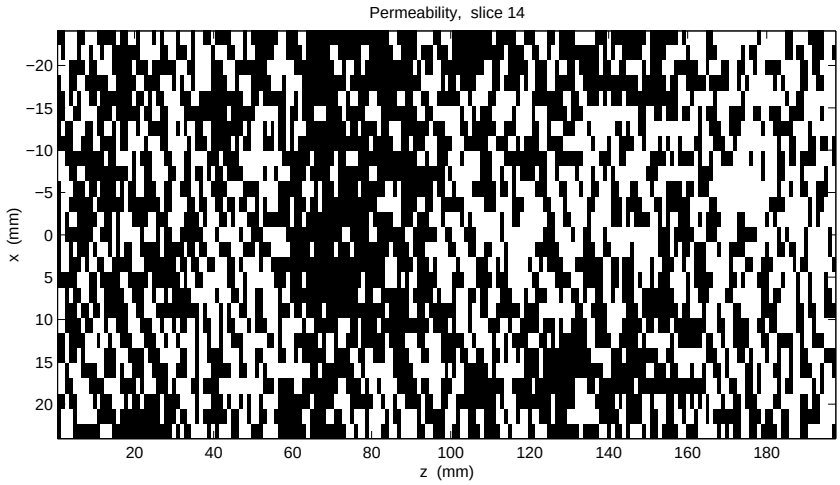

Figure 8 : a permeability longitudinal cross section obtained from the porosity map with a porosity cut-off of 0.20. Kv values are white and Km values are black.

Adjusting the permeability field

The measured dispersion were fitted by adjusting the ratio Kv/Km. Although the vug volume fraction Fv, which is given by NMR measurement, is not an adjustable parameter, we performed simulations for a different Fv to test its sensitivity on the dispersion curves. For example, at Fv=49 %, the increase of Kv/Km from 1 up to 500 does not reproduce the observed behavior (Figure 9) but only a spreading of the curves. Varying Fv within reasonable physical values and keeping Kv/Km constant yields similar results (not shown).

The experimental curves (the water case from figure 7) can be fitted by choosing the measured value of Fv (around 60%) and a ratio Kv/Km of 360 (Figure 10).

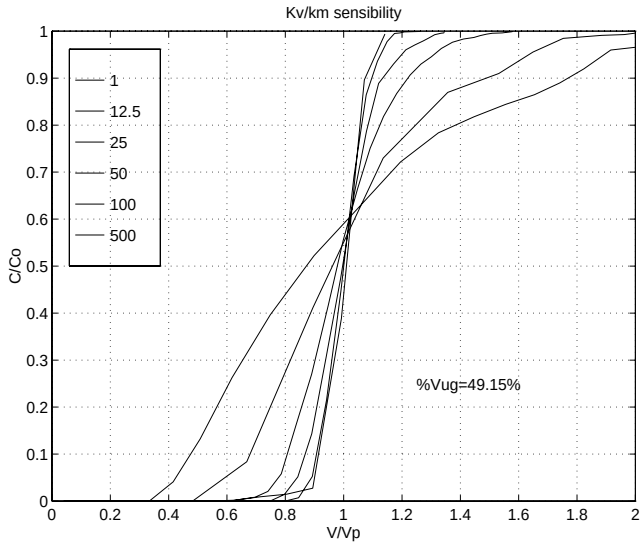

Figure 9: Simulated dispersion curves for various ratio of Kv and Km. The volume fraction was set to 49%. The larger spreading is obtained for Kv/Km=500, the smallest for Kv/Km=1.

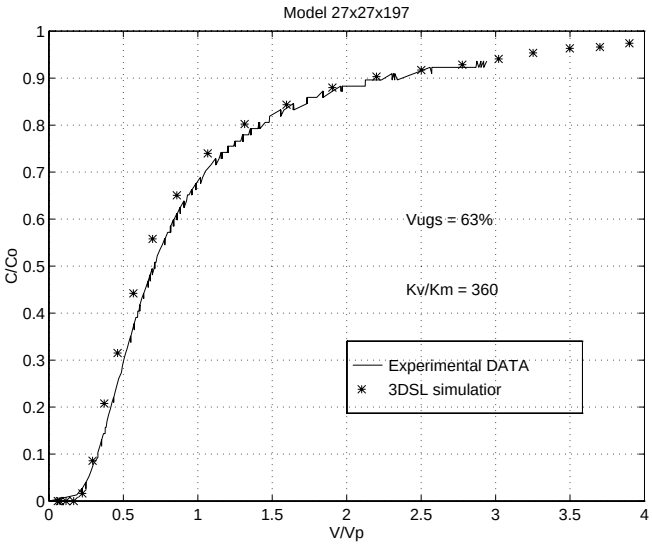

Figure 10: The experiments are best fitted for Kv/Km=360; the vug volume fraction is the one measured by NMR relaxation time.

Interpretation and discussion

The results described above indicate that the dispersion experiments can be reproduced satisfactorily by adjusting essentially one parameter Kv/Km which is indeed the most sensitive in the simulations. The vug volume fraction is not very sensitive and may vary along the sample without much impact. We propose below a simple picture of the system and try to answer three questions : (i) can we characterize the permeability structure by a single number (heterogeneity factor), (ii) what is the effect of the lack of resolution of the vug system and (iii) why the viscosity ratio does not influence the results ?

A simple picture

The experiments indicate clearly the existence of a strong preferential path, although the matrix does not contain micro-fractures, as indicated by thin section (not shown here) and by the very low average permeability of the sample. Such type of curves have been found on heterogeneous carbonates (e.g. Bretz et al., 1986) and have often been associated with the existence of large pore size distribution or micro-channels between pores. In our case, vugs are only connected through a very tight matrix. As indicated by the semi variogram analysis, the vugs are not aligned along the main flow path. The preferential path is explained in terms of fast and slow streamlines and can be summarized as follow:

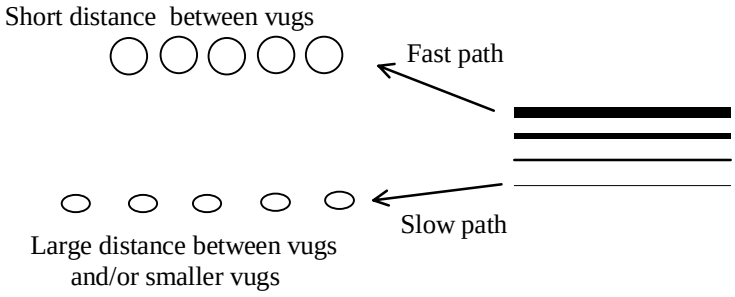

There are different fluid paths along the sample (draw as straight lines), some are fast flowing and others slow flowing paths. The fast flow lines correspond to a path where the distance between vugs is minimum. Big vugs will also be closer and amplify the effect due to a larger surface for exchange with the porous matrix . Such a path can be very tortuous in 3D space and therefor be very difficult to

visualize. The stream line simulations do partly reproduce these various paths.

Heterogeneity characterization

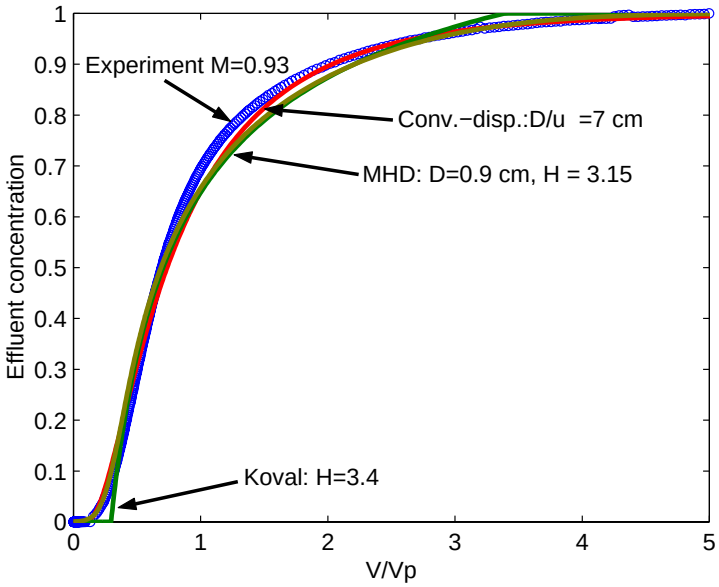

Figure 11 : Experiment for M=0.93 fitted with various models. MHD or Koval's approach are more appropriate than a convection dispersion model.

Quantification of heterogeneity is very useful to compare various samples. We tested three models predicting the effluent concentration curve as a function of one or two parameters. The detailed discussion of these models is beyond the scope of this paper and we give only the equations used, along with the physical significance. We did not considered models where molecular diffusion plays a role (e.g. Coats and Smith, 1974) because our experiments do not depend on the flow rate (which was varied by a factor of three) and therefor are not influenced by molecular diffusion. The first model consider is a standard convection-dispersion model and we used the formulation given by Brigham (1972), with flow rate imposed boundary conditions :

$$f(x,t) = \frac{1}{2} erfc\left(\frac{x-ut}{2(Dt)^{1/2}}\right) + \frac{1}{2}\exp\left(\frac{ux}{D}\right) erfc\left(\frac{x+ut}{2(Dt)^{1/2}}\right) \tag{4}$$

The dispersion coefficient D was calculated for x=L (outlet face) using standard optimization routine to find the best fit (there is no approximation performed). We found a dispersivity D/u of 7.0 cm. Despite the good fit (Figure 11), the high value obtained indicate that a convection-dispersion model cannot be used in this case because it assumes implicitly that the dispersivity must be much smaller than the sample length.

The second model that can be used is based on Koval's empirical approach (Koval, 1963). The formulation of the flux is as follows:

$$f(x,t) = \frac{H - \sqrt{Hx/ut}}{H-1} \tag{5}$$

The parameter H characterizes the degree of heterogeneity of the system and is related to the variance of permeability. The parameter H varies from 1 (homogeneous) up to 4 (layered system) for most systems. We found H=3.4 (for x=L), in agreement with the assumptions of the model.

The last model used, MHD, is a generalized approach describing the combined effect of micro (D=α/u) and macro-dispersion H, as well as viscosity (M or effective viscosity M*). The formulation used is the following (Lenormand, 1998):

$$f(x,t) = \frac{1}{4}\int_{t\min}^{t\max} \left[erfc\left(\frac{t-\bar{t}}{2\bar{t}(\alpha/x)^{1/2}}\right)+1\right] \frac{(HM^* x/u)^{1/2}}{HM^*-1} \bar{t}^{-3/2}\, d\bar{t} \tag{6}$$

We found D= 0.9 cm and H=3.15. In this case, Koval's and MHD heterogeneity parameter H are similar, as expected when H is large (Lenormand, 1998).

We conclude that Koval's or MHD approaches are adequate in this situation and the sample is well

characterized by the parameter H, obtained from models considering structure having large correlation length.

Upscaling effect

CT scan image resolution does not permit a precise description of the vugs but only a blurred spatial distribution over the sample length. For each voxel, the measured porosity is an average between vug and matrix and there are few voxels at 100 % porosity, as shown by the porosity distribution (fig. 2). From NMR measurements and considering the total sample volume, the volume fraction represented by the vugs are beyond percolation threshold (0.60x0.22=0.13). However, for the permeability map, 50% of the cells describing the sample are assigned to a high value of permeability, and therefor, these cells create a percolation path from the inlet to the outlet face. However, the early breakthrough is only reproduced for very high permeability contrast between the cells containing a large amount of matrix and cells containing a large amount of vugs. Therefor, the fitted value of 360 for the ratio Kv/Km has no specific physical significance and cannot be used to infer the average permeability of the matrix. It will depend on the choice of the size of the cells.

Viscosity effect

The most intriguing observation is the lack of viscosity effect. The viscosity ratio M was varied by a factor of 10, all fluid systems considered together, and there is no significant difference between the measured experimental curves (figure 7). Viscosity should have a stabilizing effect when M=0.3<1 and amplify the heterogeneity effect for M=3 >1. This is clearly predicted by the Koval's or MHD models where the parameter H should be replaced by the product HM (the effective viscosity ratio M* should actually be considered, not the experimental ratio M). This behavior is not only valid for viscous instability in homogeneous systems but also in a bundle of tubes with different permeabilities with a similar instability phenomenon. This observation suggests that the details of the flow through the vugs surrounded by matrix may be responsible for this effect and that H and M are not independent.

Conclusions

We studied a highly vugular, low permeability and non fractured rock and we used various techniques to characterize the porous structure both in static and dynamic ways. For static characterization: CT scan to obtain 3D porosity variations, NMR T2 measurements to obtain the vug volume fraction, variogram analysis to obtain a correlation length. For dynamic characterization : miscible displacements at two flow rates and three viscosity ratios, and streamline simulations to back calculate the permeability field.

We observed that the variogram analysis is of little significance for the sample studied because it does not predict preferential flow paths that are observed in the miscible displacement experiments.

With the help of streamline simulations, we could match the experimental results satisfactorily using a simple relation between porosity and permeability: each grid cell of the permeability field can take only two values, one associated with vugs, and one with the matrix.

We found that the heterogeneity of the sample is best described by a model designed for layered systems with large correlation length. However, the viscosity effect predicted by these models is not observed experimentally, suggesting that the details of the flow vug-matrix should be investigated.

Acknowledgments

We thank R. Lenormand and C. Barroux for their comments and suggestions, D. Fennwick for helping with the 3DSL simulator, P. Poulain and J. M. Nez for their help in the laboratory, and B. Zinsner for providing the sample.

Nomenclature

Dm : molecular diffusion

D, α : dispersion coefficient respectively in convection-dispersion equation and MHD model

Fv : vug volume percentage of the porous volume
CT : normalised CT scan number
H : heterogeneity factor in Koval's and MHD models
Kv : permeability of cells containing a large fraction of vugs
Km : permeability of cells containing a large fraction of matrix
L : sample length
M : viscosity ratio of the displaced phase to the displacing phase
r : pore radius
T2, T2b : transverse relaxation time of water in the porous space , b for bulk water
u : average pore velocity
Vp : porous volume
Φ : porosity
γ : correlation function as defined in equation 2
ρ : surface relaxivity relating time T2 to pore radius

References

Bahralolom, I.M. and Heller J.P. «Influence of Small-Scale Heterogeneities on Miscible Corefloods.» SPE/DOE 24113, presented at SPE/DOE 8th Symposium on EOR, Tulsa OK, 1992.

Batycky, R.P., Blunt, M.J. and Thiele M.R. «A 3D Field-Scale Streamline-Based Reservoir Simulator.»SPE 36726 presented at 1996 SPE Annual Technical Conference and Exhibition, Denver,Colorado, 1996.

Bretz R.E., R. Specter and F.M. Orr, 'Mixing during single phase plow in reservoir rocks: models, effects of pore structure and interpretation of experiments', Reservoir Characterization, edited by L.W. Lake and H.B. Caroll, Academic Press, 1986.

Brigham, W.E. «Mixing Equations in Short Laboratory Cores.», Paper SPE 4256 presented at SPE-AIChE Joint Symposium, Dallas TX, 1972.

Coats, K.H. and Smith, B.D. «Dead–End Pore Volume and Dispersion in Porous Media.», Society of Petroleum Engineers Journal, March 1974.

DeZabala and J. Kamath, «Laboratory evaluation of waterflood behavior of vugular carbonates». SPE 30780 presented at the Annual Technical Conference and Exhibition of SPE, Dallas, U.S.A., 1995.

Hicks, P.J., Narayanan, R. And Deans, H.A. «An Experimental Study of Miscible Displacements in Heterogeneous Carbonate Cores Using X-Ray CT». SPE 20492 presented at 65th Annual Technical Conference and Exhibition of SPE, New Orleans, LA, 1990..

Koval, E.J. «A Method for Predicting the Performance of Unstable Miscible Displacement in Heterogeneous Media», Transactions of AIME, 1963.

Lenormand, R. And Fendwick, D. «MDU:A Model for Dynamic Upscaling.» Presented at 19th IEA Collaborative on Enhanced Oil Recovery, Carmel, California, 1998.